

Anti-Cancer Properties of *Murraya koenigii* Constituent Molecules: A Computational Study

Neeta Azad

Department of Chemistry, Atma Ram Sanatan Dharma College, University of Delhi, New Delhi-110021, India

Email: [neetaazad\[at\]arsd.du.ac.in](mailto:neetaazad[at]arsd.du.ac.in)

Abstract: Carbonic Anhydrase (CA) is very essential for body cells to maintain body pH. It has different isozymes distributed across different organs of our body. Isozyme CAXII have been linked to the activity of tumor cells in various types of cancers. In this study, we aim to explore potential herbal therapeutics which can be proved to be effective in reducing the activity of CAXII isozyme and hence control activity of tumor cells. The molecules from herbs are important because they show minimum or no side effects. *Murraya koenigii* (curry leaves) constituent molecules are the centre of this study. Main eight constituent molecules of curry leaves were selected for molecular docking studies via Autodock Tools (ADT). Their various electronic properties, HOMO-LUMO, dipole moment, ESP maps, Heats of formations were calculated before going for docking studies, just to confirm their stability and reactivity. Further to check their druglikeness, Swiss ADME platform was used to scan their ADME profile. Finally, all the geometry optimized ligands were docked into the prepared protein CAXII. The results obtained were promising. Binding affinity of -6.9 Kcal/mol for M6 and -6.4 Kcal/mol for M8 were quite acceptable, which shows both these ligands can be further analysed for their good inhibiting properties towards CAXII to suppress the activity of tumor cells.

Keywords: Autodock, SwissADME, Cancer Cells, Carbonic anhydrase, Curry leaves, Molecular Docking

1. Introduction

Carbonic anhydrase (CA) is an enzyme crucial for maintaining pH balance during ion exchange in various physiological processes such as digestion, respiration, renal function, and bone resorption. CAs are found ubiquitously in both prokaryotes and eukaryotes, and they are differentiated into four gene families: α -CAs, β -CAs, γ -CAs, and δ -CAs [1], [2]. In humans, only α -CAs exist, represented by 14 isoforms (CA I to CA IVX), with organ-specific distribution (8-10). The primary function of CAs is to catalyze the conversion of CO₂ to carbonic acid and protons to maintain a balanced pH [1], [3].

In cancer cells, abnormal metabolism requires high energy to sustain rapid cell multiplication, fulfilled by bicarbonate ions produced with the help of CA. This study specifically focuses on α -CAs. Investigations reveal that among the various isoforms, CAIX and CAXII are associated with tumor growth [2], [3], [4], while isoforms CA I, CA II, CA III, and CA XIII are associated with normal tissues [1], [5]. Consequently, this computational study concentrates on CAXII.

Murraya koenigii (L.) Spreng, commonly known as curry leaf, belongs to the Rutaceae family and is native to India, now distributed in Southern and Southeast Asia [6]. Curry leaves, or curry patta, are integral to Indian cuisine due to their health-promoting properties. In Ayurveda, curry leaves hold significance for their curative properties related to skin diseases, cough and cold, hysteria, rheumatism, hypertension [7], antioxidant [8], anti-inflammatory [8], antihyperglycemic [9], and hypoglycemic effects [10]. While limited research has been conducted on curry leaves' anticancer properties, some studies suggest that various constituent molecules of *Murraya koenigii* may act as effective anticancer therapeutics [11].

This study explores the inhibitory potential of constituent molecules from curry leaves against CAXII. The ADME

profile of the ligands was assessed using Swiss ADME [12]. Crystal structure of CAXII were obtained from the Research Collaboratory for Structural Bioinformatics (RCSB) Protein Data Bank (www.rcsb.org) with PDB ID 1JCZ. Protein structure underwent a 'protein preparation step' to make them ready for docking in BIOVIA discovery studio [13], and ligand structures were drawn and geometry optimized in ArgusLab [14].

2. Methodology and computational details

Molecular docking method has been adopted in the present study [15], [16]. The interaction of CAXII has been investigated with eight important constituent molecules (ligands) of *Murraya Koenigii* [17]. Both protein and ligands were subjected to systematic preparation before barging into the molecular docking study. The docking scores of each ligand and their binding with the protein was analysed by comparing various electronic properties of ligands. ADME profile and drug likeness of the all ligands was checked with the help of SwissADME.

2.1 Protein preparation

This step is of prime importance which ensures the removal of extra protein chains in the downloaded structure of target protein, removal of water molecules to avoid undesirable interactions between ligand and water molecules. This step also involves the detection of any missing chains in the protein and locating the binding site for target specific docking.

The desired target protein, Carbonic anhydrase XII (CAXII) was imported from the Research Collaboratory for Structural Bioinformatics (RCSB) Protein Data Bank (www.rcsb.org) with PDB ID: 1JCZ. BIOVIA Discovery Studio software [13] was used for protein preparation. There were two chains present in the downloaded protein pdb file. Chain B was deleted along with all water molecules to make protein

structure simplified and ready for docking. Ligands, Acetic acid and Zinc ion were present in the binding pocket of chain A of the protein. These both ligands were deleted as we aimed for blind docking in the present study. The grid box was centred at $x = 16.6078$, $y = 0.000$, $z = 26.7452$ and the size of grid box was $x = 29.74$ Å, $y = 25.00$ Å, $z = 35.73$ Å.

2.2 Ligand preparation

The structures of all the ligands were drawn and optimized in ArgusLab software. before optimizing their geometries using Quantum Mechanical method, all geometries were energy minimized using Molecular Mechanics UFF (Universal force

field) method. Quantum Mechanical method AM1 was used for geometry optimization after cleaning geometry of each ligand via UFF. Energy minimization was done using BFGS and Restricted Hartree Fock (RHF) method was selected for closed shell consideration of electrons. Along with geometry optimization various electronic properties, like dipole moment, Highest occupied molecular orbitals (HOMO), Lowest Unoccupied Molecular Orbitals (LUMO), Mulliken Charges, dipole moments, Heats of formation and Electrostatic Potential Maps (ESP) were calculated for comparison of stability of each ligand. Optimized structures of all the ligands have been mentioned in figure 1.

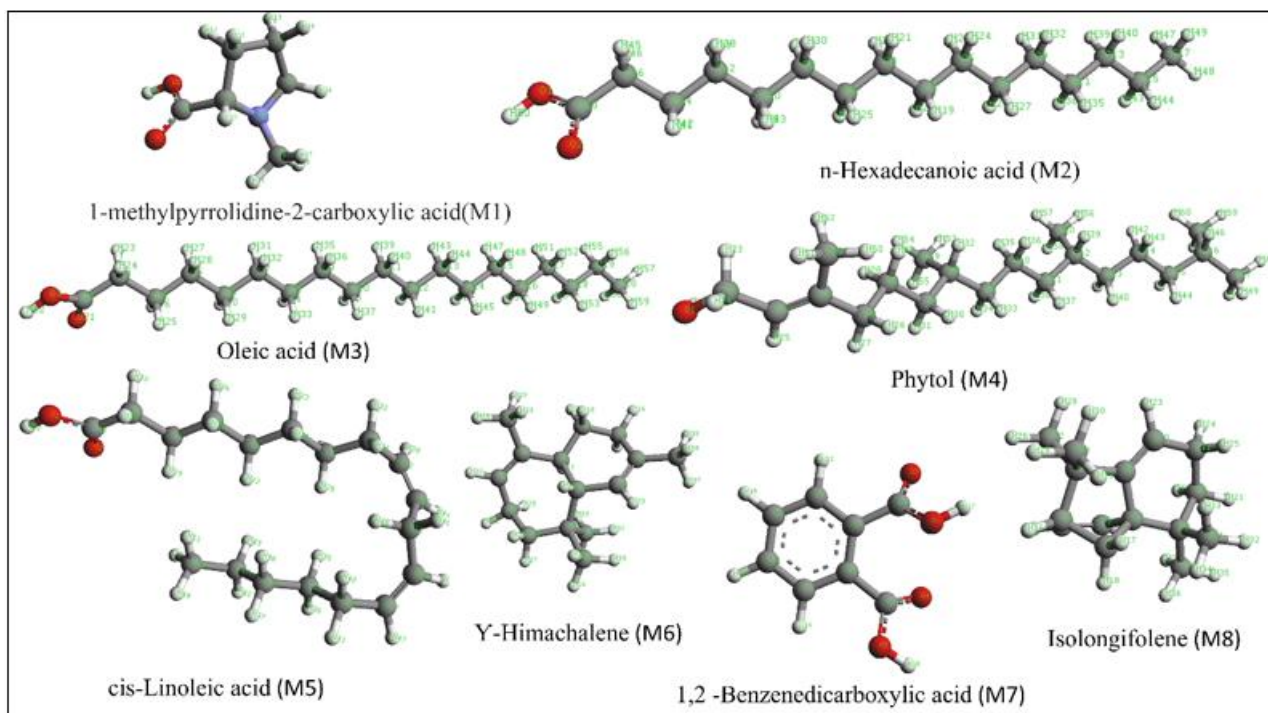


Figure 1: Geometry optimized structures (by AM1) of Important constituent molecules of Curry leaves considered for present studies

2.3 Molecular Docking

When ligands and protein (CAXII) were ready for docking. The files were imported to Autodock Vina [18] and docking was performed via Pyrex. The grid was generated around the defined docking site and docking was performed. Each ligand got docking score against several conformations within the protein binding pocket.

3. Result and Discussion

3.1 Ligand's Calculated Properties

The important electronic properties of all these eight molecules named M1 to M8 were calculated to check their relative stability and reactivity (Table 1). Optimized geometries of these ligands are displayed in figure 1. Calculated properties were helpful in determining how the ligand can behave within the binding pocket of protein. Looking at the heats of formations of these molecules M3 is the most stable one with $\Delta H_f = -212$ Kcal/mol and M8 is the least stable with positive heat of formation i.e. 30.747

Kcal/mol. The order of stability of these molecules on the basis of their heats of formation can be given as:
 $M3 > M2 > M7 > M5 > M4 > M1 > M6 > M8$

Energies of highest occupied molecular orbitals (HOMO) and lowest unoccupied molecular orbitals (LUMO) were calculated to have an idea about how easily the electron transfer can happen in case of binding with the amino acids of the protein binding sites. The $\Delta E = E_{LUMO} - E_{HOMO}$ energy was found to be maximum for M2 and minimum for M7. Which tells about the possibility of easy transfer of electrons from HOMO to LUMO whenever needed during binding with protein. The order of $\Delta E = E_{LUMO} - E_{HOMO}$ is found to be $M2 > M3 > M1 > M5 > M4 > M6 = M8 > M7$. Here as per HOMO-LUMO gap M6 and M8 are equally reactive. Dipole moments of these molecules were calculated to check upon the polar nature of these ligand candidates. More polar the molecule is better is its solubility in polar solvents. Also, existing dipole moment of molecules help them to form hydrogen bonds with the amino acids of protein for better binding and forming a stable protein-ligand complex. As per calculated values mentioned in table 1 M7 has highest dipole

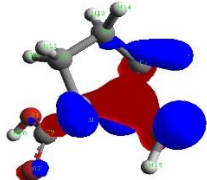
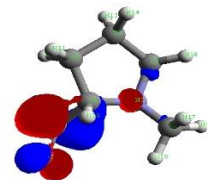
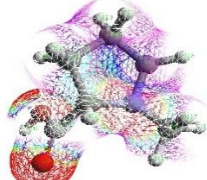
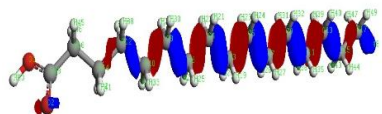
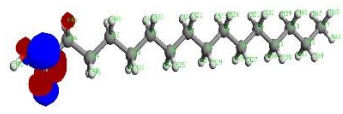
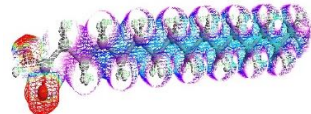
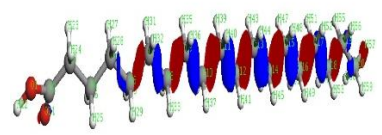

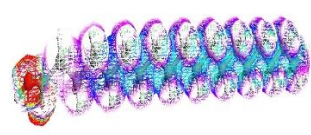
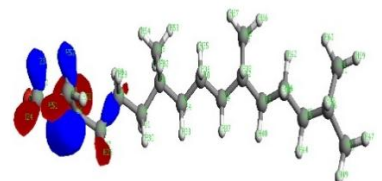
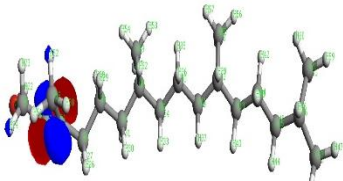
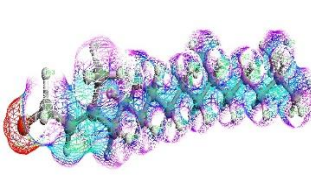
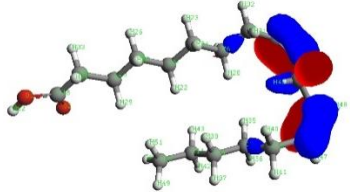
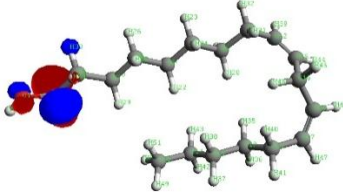
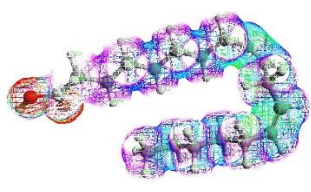
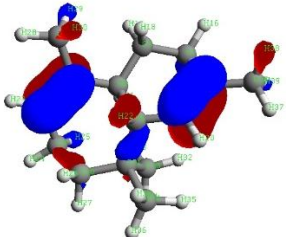
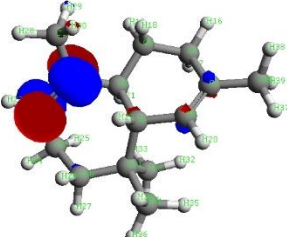
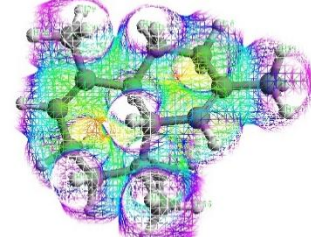
moment. M6 and M8 are least polar molecules and rest of the molecules possess moderate dipole moments.

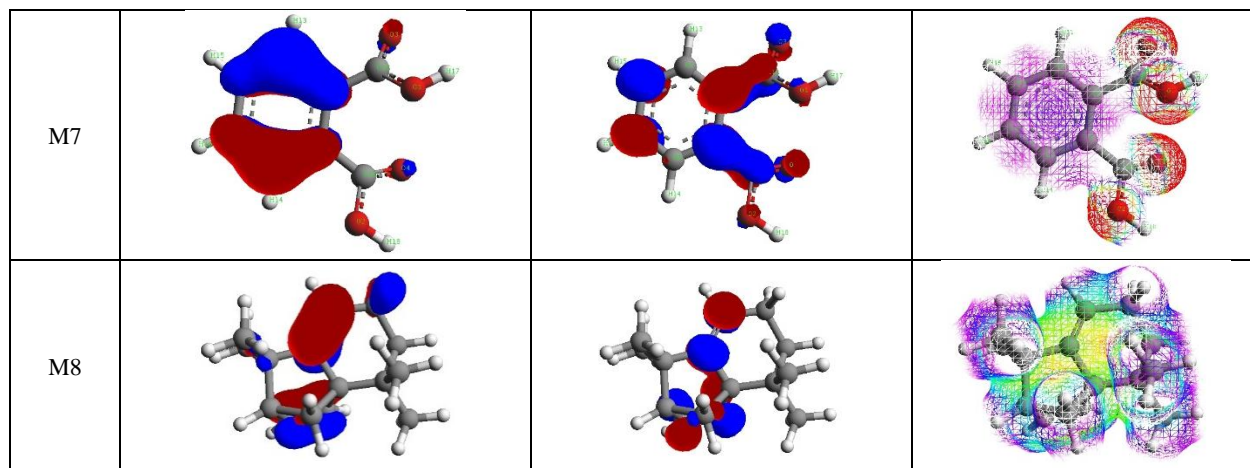
In table 2 HOMOs and LUMOs of all ligands along with their ESP maps are shown. The pictorial representations of HOMO-LUMO makes it easier to understand, which sites are electron rich and which ones are electron deficient for electrophilic or nucleophilic attacks. ESP maps clearly show the electron density on each atom in form of colour coding. Red colour indicates the high electron density and it dissipates as the colour transits from red to blue. The white colour shows neutral sites in a molecule. The red sites can play significant role as hydrogen bond acceptors due to high electron density and blue sites can be helpful as hydrogen bond acceptors for electron donating groups.

Table 1: Various electronic properties of the ligands

Ligand	Heats of formation (ΔH_f Kcal/mol)	E_{HOMO}	E_{LUMO}	$\Delta E = E_{LUMO} - E_{HOMO}$	Dipole Moment (Debye)
		(Kcal/mol)	(Kcal/mol)		
M1	-91.947	-0.350	0.041	0.391	2.812
M2	-192.569	-0.405	0.038	0.443	1.896
M3	-212.044	-0.402	0.038	0.440	1.900
M4	-141.161	-0.351	0.035	0.386	2.037
M5	-146.374	-0.350	0.038	0.388	1.773
M6	-13.190	-0.337	0.046	0.383	0.271
M7	-148.866	-0.386	-0.033	0.352	3.655
M8	30.747	-0.340	0.043	0.383	0.168

Table 2: HOMO-LUMO and Electrostatic Potential Maps (ESP) plots of ligands

Ligand	HOMO	LUMO	ESP maps
M1			
M2			
M3			
M4			
M5			
M6			

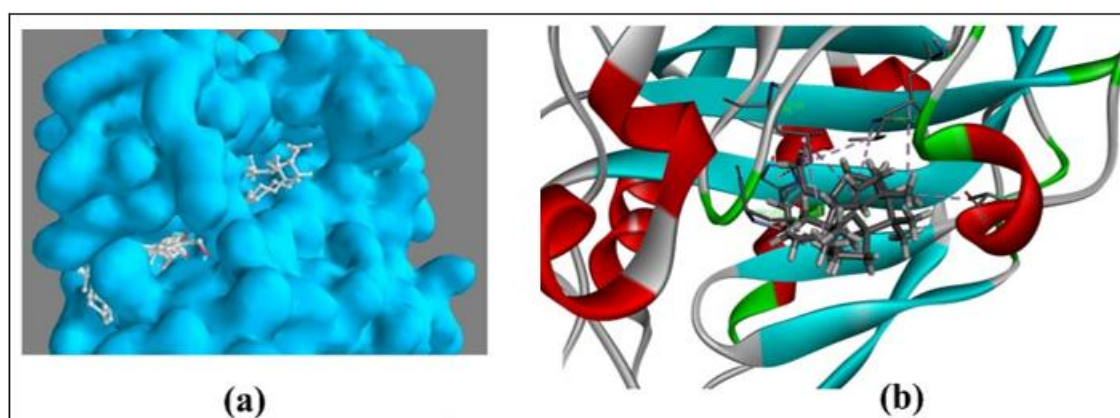


3.2 Docking Results

Molecular docking is an effective way of studying the possible favourable and non-favourable interactions between ligand and receptor. If the binding score for ligand-receptor complex is not good, binding is very unlikely. Molecular docking was done for the selected molecules and protein receptor carbonic anhydrase XII isozyme (CAXII). Ligands were docked to the prepared protein CAXII and the docked protein-ligand complex was imported into discovery studio for binding mode analysis.

Blind docking was adopted for this study. The grid box was centred at $x = 16.6078$, $y = 0.000$, $z = 26.7452$ and the size of grid box was adjusted at $x = 29.74 \text{ \AA}$, $y = 25.00 \text{ \AA}$, $z = 35.73 \text{ \AA}$, so that the entire protein could come inside the grid box and all possible binding sites can be covered. All ligands form different conformations within the cavity of protein to get best fitted conformation. The docking scores against each conformation of all 8 ligands has been mentioned in table S1 of supplementary information. And scores of best conformation of each ligand has been mentioned in table 3. Ligand 6 (M6) and Ligand 8 (M8) had shown best docking scores, hence their best poses were exported to BIOVIA discovery studio and analysed. In Figure 2 (a) the space filling model of the protein has been displayed. Here it is clearly

visible that different ligands have chosen different binding sites depending upon their interactions with respective amino acids in target protein. In figure 2 (b) M6 and M8 have been made visible in the cavity of protein. This shows both these ligands bind at the same binding site of protein. Figure 2 (c) and (d) shows interactions of M6 and M8 respectively with protein residues. In both the cases mainly allyl (pink coloured) interactions are playing major role in making ligands and protein intact in the binding pocket. Green coloured sites are the ones which are creating Van der Waals interactions with the ligands. For M6 important binding residues are ALA 131, PRO202, SER135, SER132, THR91, LEU141, GLN92, VAL121, LEU198, THR199, HIS94, THR200, LYS67, TRP5 and PRO201. For M8 the important binding residue are VAL121, LEU141, ALA131, PRO202 and LEU198. Ligand M6 is bind to the protein more firmly and shows better interactions and docking score of -6.9 Kcal/mol , due to involvement of allyl as well as Van der Waals interactions. On the other hand, ligand M8 shows weaker interactions with docking score of -6.4 Kcal/mol due to lack of any other important interactions like hydrogen donor acceptor or Van der Waals etc. rest of the ligands show poorer docking scores as compared to these two ligands. This shows M6 and M8 can be better binders or inhibitors for CAXII protein.



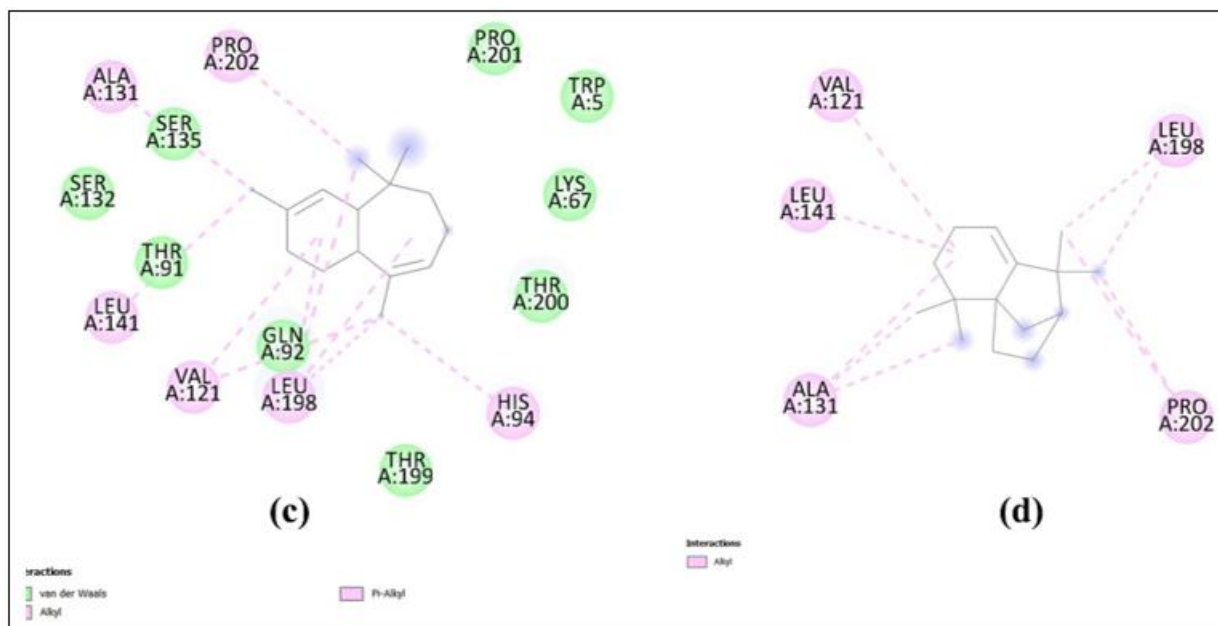


Figure 2: Molecular docking images of ligand 6 and 8 (a) Space filling model of protein and ligands binding at different sites during blind docking. (b) Ligand 6 and 8 present in the same cavity of protein (c) & (d) Various bonding residues of protein i

3.3 ADME properties

ADME (Adsorption, Distribution, Metabolism and Excretion) profile is important to describe various pharmacokinetic properties and Drug likeness of ligands. SwissADME was used to calculate various drug like properties of the ligands undertaken for this study and verify whether these hits follow Lipinski's rule of five.

All SwissADME properties have been reported in table S2 of supplementary information. A few important ones are mentioned in table 3 below. Ligands M6 and M8 don't have any hydrogen donor or acceptor groups. Also, their Gastrointestinal absorption score is low. Blood brain barrier (BBB) permeant is no for both and their bioavailability score is around 55%. Talking about Lipinski's rule of five violation both of these ligands violate 2 Lipinski's rule each. All these parameters indicate their moderately active properties towards druglikeness.

Table 3: Molecular docking score and ADME results for the ligands under investigation

Molecule	Binding Energy (KJ/mol)	#H-bond acceptors	#H-bond donors	GI absorption	BBB permeant	Lipinski #violations	Bioavailability Score	Leadlikeness #violations
M 1	-4.8	3	1	High	No	0	0.55	1
M 2	-5.3	2	1	High	Yes	1	0.85	2
M 3	-5.2	2	1	High	No	1	0.85	2
M 4	-5.6	1	1	Low	No	1	0.55	2
M 5	-5.7	2	1	High	Yes	1	0.85	2
M 6	-6.9	0	0	Low	No	1	0.55	2
M 7	-5.8	4	2	High	No	0	0.85	1
M 8	-6.4	0	0	Low	No	1	0.55	2

4. Conclusions

In Indian culinary traditions, curry leaves play a vital role, not only for their flavor but also for their numerous health benefits. Recent docking studies have highlighted those two key compounds found in curry leaves, γ -Himachalene and Isolongifolene, may be effective in controlling tumor growth. These molecules exhibit favourable binding energies that can inhibit carbonic anhydrase, an enzyme associated with cancer progression. By forming stable complexes with Carbonic Anhydrase XII and blocking its potential binding sites, these compounds interfere with the energy supply to cancerous cells, thereby inhibiting tumor growth.

Incorporating curry leaves into one's daily diet is a simple and natural way to help prevent tumor. Organically grown

Murraya koenigii, or curry leaves, are particularly beneficial as they avoid the risks associated with pesticide exposure. To promote this, the practice of growing curry leaves at home should be encouraged, along with educating people about their health benefits by drawing on examples from traditional culinary practices.

References

- [1] T. Stams and D. W. Christianson, "X-ray crystallographic studies of mammalian carbonic anhydrase isozymes," in *The Carbonic Anhydrases*, Basel: Birkhäuser Basel, 2000, pp. 159–174. doi: 10.1007/978-3-0348-8446-4_9.
- [2] S. Pastorekova, S. Parkkila, J. Pastorek, and C. T. Supuran, "Review Article," *J Enzyme Inhib Med*

- Chem*, vol. 19, no. 3, pp. 199–229, Jan. 2004, doi: 10.1080/14756360410001689540.
- [3] C. T. Supuran, A. Scozzafava, and A. Casini, “Carbonic anhydrase inhibitors,” *Med Res Rev*, vol. 23, no. 2, pp. 146–189, Mar. 2003, doi: 10.1002/med.10025.
- [4] Z. Chen *et al.*, “Differential expression and function of CAIX and CAXII in breast cancer: A comparison between tumorgraft models and cells,” *PLoS One*, vol. 13, no. 7, p. e0199476, Jul. 2018, doi: 10.1371/journal.pone.0199476.
- [5] D. Hewett-Emmett, “Evolution and distribution of the carbonic anhydrase gene families,” in *The Carbonic Anhydrases*, Basel: Birkhäuser Basel, 2000, pp. 29–76. doi: 10.1007/978-3-0348-8446-4_3.
- [6] S. Chand Saini and G. Bala Show Reddy, “A Review on Curry Leaves (*Murraya koenigii*): Versatile Multi-Potential Medicinal Plant.” [Online]. Available: www.ajpct.org
- [7] C. Ito *et al.*, “Induction of apoptosis by carbazole alkaloids isolated from *Murraya koenigii*,” *Phytomedicine*, vol. 13, no. 5, pp. 359–365, May 2006, doi: 10.1016/j.phymed.2005.03.010.
- [8] F. Mohd Nor, M. Suhaila, I. Nor Aini, and I. Razali, “Antioxidative properties of *Murraya koenigii* leaf extracts in accelerated oxidation and deep-frying studies,” *Int J Food Sci Nutr*, vol. 60, no. sup2, pp. 1–11, Jan. 2009, doi: 10.1080/09637480802158168.
- [9] B. Dineshkumar, A. Mitra, and M. Mahadevappa, “Antidiabetic and hypolipidemic effects of mahanimbine (carbazole alkaloid) from *Murraya koenigii* (rutaceae) leaves,” *International Journal of Phytomedicine*, vol. 2, no. 1, pp. 22–30, 2010, doi: 10.5138/ijpm.2010.0975.0185.02004.
- [10] T. S. V and S. D. M, “HYPOGLYCEMIC EFFECTS OF FRUIT JUICE OF MURRAYA KOENIGII (L) IN ALLOXAN INDUCED DIABETIC MICE.”
- [11] A. Ghasemzadeh, H. Z. E. Jaafar, A. Rahmat, and T. Devarajan, “Evaluation of Bioactive Compounds, Pharmaceutical Quality, and Anticancer Activity of Curry Leaf (*Murraya koenigii* L.),” *Evidence-Based Complementary and Alternative Medicine*, vol. 2014, no. 1, Jan. 2014, doi: 10.1155/2014/873803.
- [12] A. Daina, O. Michielin, and V. Zoete, “SwissADME: a free web tool to evaluate pharmacokinetics, drug-likeness and medicinal chemistry friendliness of small molecules,” *Sci Rep*, vol. 7, no. 1, p. 42717, Mar. 2017, doi: 10.1038/srep42717.
- [13] <https://www.3ds.com/products-services/BIOVIA/products/molecular-modeling-simulation/BIOVIA-discovery-studio/visualization>. (n.d.).
- [14] A. S. Achutha, V. L. Pushpa, and K. B. Manoj, “Comparative molecular docking studies of phytochemicals as Jak2 inhibitors using Autodock and ArgusLab,” *Mater Today Proc*, vol. 41, pp. 711–716, 2021, doi: 10.1016/j.matpr.2020.05.661.
- [15] N. Azad, M. Bhandari, and R. Kakkar, “Discovery of Some Potent PDHK Inhibitors Using Pharmacophore Modeling, Virtual Screening and Molecular Docking Studies Discovery of some potent PDHK inhibitors using pharmacophore modeling, virtual screening and molecular docking studies,” *Journal of Biochemistry and Molecular Biology Research*, vol. 2, no. 1, pp. 67–72, 2016, doi: 10.17554/j.issn.1239-6518.2016.02.12.
- [16] N. Azad, N. Sharma, E. Arora, and P. Gupta, “In silico analysis of interaction of Eugenol, cis-Isoeugenol and Methyl Eugenol with the binding site of spike protein of SARS-CoV19 virus,” 2024.
- [17] R. Hema, S. Kumaravel, and K. Alagusundaram, “GC/MS Determination of Bioactive Components of *Murraya koenigii*,” 2011. [Online]. Available: <http://www.americanscience.org><http://www.americanscience.org>
- [18] <https://autodock.scripps.edu/>. (n.d.)

Supplementary Information

Table: S1 Binding Affinities for various conformations of ligands M1 to M8 inside the protein cavity

Different conformations of Ligands complexed with CAXII	Binding Affinity (Kcal/mol)	rmsd/ub	rmsd/lb
1jcz-CAXIIprep_ligand1_uff_E=202.41	-4.8	0	0
1jcz-CAXIIprep_ligand1_uff_E=202.41	-4.7	3.081	2.307
1jcz-CAXIIprep_ligand1_uff_E=202.41	-4.6	3.053	2.079
1jcz-CAXIIprep_ligand1_uff_E=202.41	-4.6	2.409	1.24
1jcz-CAXIIprep_ligand1_uff_E=202.41	-4.5	3.616	3.026
1jcz-CAXIIprep_ligand1_uff_E=202.41	-4.5	3.297	2.208
1jcz-CAXIIprep_ligand1_uff_E=202.41	-4.4	27.499	26.718
1jcz-CAXIIprep_ligand1_uff_E=202.41	-4.4	14.474	13.656
1jcz-CAXIIprep_ligand1_uff_E=202.41	-4.3	23.473	22.974
1jcz-CAXIIprep_ligand2_uff_E=57.46	-5.3	0	0
1jcz-CAXIIprep_ligand2_uff_E=57.46	-5.1	6.234	3.855
1jcz-CAXIIprep_ligand2_uff_E=57.46	-5	14.782	11.716
1jcz-CAXIIprep_ligand2_uff_E=57.46	-4.9	33.163	30.323
1jcz-CAXIIprep_ligand2_uff_E=57.46	-4.9	7.708	4.465
1jcz-CAXIIprep_ligand2_uff_E=57.46	-4.9	16.833	13.698
1jcz-CAXIIprep_ligand2_uff_E=57.46	-4.8	5.313	3.254
1jcz-CAXIIprep_ligand2_uff_E=57.46	-4.8	8.868	5.803
1jcz-CAXIIprep_ligand2_uff_E=57.46	-4.8	15.284	11.989
1jcz-CAXIIprep_ligand3_uff_E=121.35	-5.2	0	0
1jcz-CAXIIprep_ligand3_uff_E=121.35	-5.2	4.64	1.777

lcz-CAXIIPrep_ligand3_uff_E=121.35	-5.1	18.338	13.866
lcz-CAXIIPrep_ligand3_uff_E=121.35	-5	6.429	2.847
lcz-CAXIIPrep_ligand3_uff_E=121.35	-5	19.38	14.809
lcz-CAXIIPrep_ligand3_uff_E=121.35	-4.9	4.604	1.608
lcz-CAXIIPrep_ligand3_uff_E=121.35	-4.8	3.393	2.242
lcz-CAXIIPrep_ligand3_uff_E=121.35	-4.8	17.419	13.439
lcz-CAXIIPrep_ligand3_uff_E=121.35	-4.7	18.512	13.928
lcz-CAXIIPrep_Ligand4_uff_E=199.21	-5.6	0	0
lcz-CAXIIPrep_Ligand4_uff_E=199.21	-5.6	4.495	2.36
lcz-CAXIIPrep_Ligand4_uff_E=199.21	-5.6	6.618	2.78
lcz-CAXIIPrep_Ligand4_uff_E=199.21	-5.5	17.599	12.843
lcz-CAXIIPrep_Ligand4_uff_E=199.21	-5.5	1.962	1.118
lcz-CAXIIPrep_Ligand4_uff_E=199.21	-5.4	2.646	1.798
lcz-CAXIIPrep_Ligand4_uff_E=199.21	-5.3	3.892	1.526
lcz-CAXIIPrep_Ligand4_uff_E=199.21	-5.3	5.804	2.516
lcz-CAXIIPrep_Ligand4_uff_E=199.21	-5.3	18.903	14.713
lcz-CAXIIPrep_ligand5_uff_E=147.85	-5.7	0	0
lcz-CAXIIPrep_ligand5_uff_E=147.85	-5.6	16.185	12.827
lcz-CAXIIPrep_ligand5_uff_E=147.85	-5.5	16.961	13.181
lcz-CAXIIPrep_ligand5_uff_E=147.85	-5.4	19.483	15.528
lcz-CAXIIPrep_ligand5_uff_E=147.85	-5.4	6.692	3.871
lcz-CAXIIPrep_ligand5_uff_E=147.85	-5.4	5.743	4.215
lcz-CAXIIPrep_ligand5_uff_E=147.85	-5.3	18.668	14.955
lcz-CAXIIPrep_ligand5_uff_E=147.85	-5.3	17.404	14.027
lcz-CAXIIPrep_ligand5_uff_E=147.85	-5.3	6.382	3.675
lcz-CAXIIPrep_ligand6_uff_E=252.33	-6.9	0	0
lcz-CAXIIPrep_ligand6_uff_E=252.33	-6.4	1.501	1.081
lcz-CAXIIPrep_ligand6_uff_E=252.33	-6.2	4.106	1.076
lcz-CAXIIPrep_ligand6_uff_E=252.33	-6	2.312	1.587
lcz-CAXIIPrep_ligand6_uff_E=252.33	-5.8	3.836	2.267
lcz-CAXIIPrep_ligand6_uff_E=252.33	-5.8	5.02	1.903
lcz-CAXIIPrep_ligand6_uff_E=252.33	-5.5	18.003	14.536
lcz-CAXIIPrep_ligand6_uff_E=252.33	-5.4	16.625	14.317
lcz-CAXIIPrep_ligand6_uff_E=252.33	-5.3	18.662	15.996
lcz-CAXIIPrep_ligand7_uff_E=150.70	-5.8	0	0
lcz-CAXIIPrep_ligand7_uff_E=150.70	-5.8	2.611	1.546
lcz-CAXIIPrep_ligand7_uff_E=150.70	-5.8	3.189	0.057
lcz-CAXIIPrep_ligand7_uff_E=150.70	-5.8	3.462	1.535
lcz-CAXIIPrep_ligand7_uff_E=150.70	-5.7	15.423	13.775
lcz-CAXIIPrep_ligand7_uff_E=150.70	-5.5	6.108	4.319
lcz-CAXIIPrep_ligand7_uff_E=150.70	-5.5	5.781	4.312
lcz-CAXIIPrep_ligand7_uff_E=150.70	-5.2	11.741	10.075
lcz-CAXIIPrep_ligand7_uff_E=150.70	-5.2	5.482	3.835
lcz-CAXIIPrep_ligand8_uff_E=463.56	-6.4	0	0
lcz-CAXIIPrep_ligand8_uff_E=463.56	-5.8	5	1.968
lcz-CAXIIPrep_ligand8_uff_E=463.56	-5.5	3.957	1.041
lcz-CAXIIPrep_ligand8_uff_E=463.56	-5.4	4.532	1.155
lcz-CAXIIPrep_ligand8_uff_E=463.56	-5.3	4.508	1.294
lcz-CAXIIPrep_ligand8_uff_E=463.56	-5.2	27.294	24.552
lcz-CAXIIPrep_ligand8_uff_E=463.56	-5.2	21.165	18.613
lcz-CAXIIPrep_ligand8_uff_E=463.56	-5.2	20.649	18.07
lcz-CAXIIPrep_ligand8_uff_E=463.56	-5.2	21.474	18.999

Table: S2 Various ADME properties of ligands calculated by SwissADME

Molecule	Molecule 1	Molecule 2	Molecule 3	Molecule 4	Molecule 5	Molecule 6	Molecule 7	Molecule 8
Canonical SMILES	CN1CCC1C(=O)O	CCCCCCCC(=O)O	CCCCCCCC(=O)O	OCC=C(CCCC(C)C)C	CCCCC=CCC(=O)O	CC1=CC2C(CC1)C(=CCCC2(C)C)C	OC(=O)c1ccccc1C(=O)O	CC1(C)C2C=CC3(C1=CCCC3(C)C)C2
Formula	C6H11NO2	C16H32O2	C18H34O2	C20H40O	C18H32O2	C15H24	C8H6O4	C15H22
MW	129.16	256.42	282.46	296.53	280.45	204.35	166.13	202.34
#Heavy atoms	9	18	20	21	20	15	12	15
#Aromatic heavy atoms	0	0	0	0	0	0	6	0

Fraction Csp3	0.83	0.94	0.83	0.9	0.72	0.73	0	0.73
#Rotatable bonds	1	14	15	13	14	0	2	0
#H-bond acceptors	3	2	2	1	2	0	4	0
#H-bond donors	1	1	1	1	1	0	2	0
MR	37.42	80.8	89.94	98.94	89.46	68.78	40.36	66.15
TPSA	40.54	37.3	37.3	20.23	37.3	0	74.6	0
iLOGP	1.31	3.85	4.27	4.71	4.14	3.26	0.6	3.09
XLOGP3	-3	7.17	7.64	8.19	6.98	4.22	0.73	4.56
WLOGP	-0.22	5.55	6.11	6.36	5.88	4.73	1.08	4.34
MLOGP	0	4.19	4.57	5.25	4.47	4.63	1.2	4.63
Silicos-IT Log P	0.04	5.25	5.95	6.57	5.77	3.91	0.61	3.9
Consensus Log P	-0.37	5.2	5.71	6.22	5.45	4.15	0.84	4.1
ESOL Log S	1.32	-5.02	-5.41	-5.98	-5.05	-3.77	-1.57	-3.97
ESOL Solubility (mg/ml)	2.67E+03	2.43E-03	1.09E-03	3.10E-04	2.49E-03	3.51E-02	4.49E+00	2.18E-02
ESOL Solubility (mol/l)	2.07E+01	9.49E-06	3.85E-06	1.05E-06	8.87E-06	1.72E-04	2.70E-02	1.08E-04
ESOL Class	Highly soluble	Moderately soluble	Moderately soluble	Moderately soluble	Moderately soluble	Soluble	Very soluble	Soluble
Ali Log S	2.71	-7.77	-8.26	-8.47	-7.58	-3.93	-1.88	-4.28
Ali Solubility (mg/ml)	6.63E+04	4.31E-06	1.54E-06	9.94E-07	7.42E-06	2.40E-02	2.21E+00	1.05E-02
Ali Solubility (mol/l)	5.14E+02	1.68E-08	5.46E-09	3.35E-09	2.64E-08	1.17E-04	1.33E-02	5.21E-05
Ali Class	Highly soluble	Poorly soluble	Poorly soluble	Poorly soluble	Poorly soluble	Soluble	Very soluble	Moderately soluble
Silicos-IT LogSw	0.18	-5.31	-5.39	-5.51	-4.67	-3.52	-1.14	-3.5
Silicos-IT Solubility (mg/ml)	1.96E+02	1.25E-03	1.14E-03	9.06E-04	5.93E-03	6.19E-02	1.21E+01	6.40E-02
Silicos-IT Solubility (mol/l)	1.52E+00	4.88E-06	4.04E-06	3.05E-06	2.11E-05	3.03E-04	7.29E-02	3.16E-04
Silicos-IT class	Soluble	Moderately soluble	Moderately soluble	Moderately soluble	Moderately soluble	Soluble	Soluble	Soluble
GI absorption	High	High	High	Low	High	Low	High	Low
BBB permeant	No	Yes	No	No	Yes	No	No	No
Pgp substrate	No	No	No	Yes	No	No	No	No
CYP1A2 inhibitor	No	Yes	Yes	No	Yes	No	No	No
CYP2C19 inhibitor	No	No	No	No	No	Yes	No	Yes
CYP2C9 inhibitor	No	Yes	Yes	Yes	Yes	Yes	No	Yes
CYP2D6 inhibitor	No	No	No	No	No	No	No	No
CYP3A4 inhibitor	No	No	No	No	No	No	No	No
log Kp (cm/s)	-9.22	-2.77	-2.6	-2.29	-3.05	-4.55	-6.8	-4.3
Lipinski #violations	0	1	1	1	1	1	0	1
Ghose #violations	2	0	1	1	1	0	1	0
Veber #violations	0	1	1	1	1	0	0	0

Egan #violations	0	0	1	1	1	0	0	0
Muegge #violations	2	1	1	2	1	1	1	1
Bioavailability Score	0.55	0.85	0.85	0.55	0.85	0.55	0.85	0.55
PAINS #alerts	0	0	0	0	0	0	0	0
Brenk #alerts	0	0	1	1	1	1	0	1
Leadlikeness #violations	1	2	2	2	2	2	1	2
Synthetic Accessibility	1.63	2.31	3.07	4.3	3.1	4.38	1	5.32